AGU PUBLICATIONS

Geophysical Research Letters

RESEARCH LETTER
10.1002/2014GL062443

Key Points:
- Source-specific optical properties evaluated in different model approaches
- Particle morphology is major model sensitivity
- This sensitivity is acute for larger BC core and thicker coating thickness

Supporting Information:
- Sections S1–S5 and Figures S1–S5

Correspondence to:
D. Liu,
Dantong.liu@manchester.ac.uk

Citation:
Liu, D., J. W. Taylor, D. E. Young, M. J. Flynn, H. Coe, and J. D. Allan (2015), The effect of complex black carbon microphysics on the determination of the optical properties of brown carbon, *Geophys. Res. Lett.*, *42*, 613–619, doi:10.1002/2014GL062443.

Received 4 NOV 2014
Accepted 29 DEC 2014
Accepted article online 7 JAN 2015
Published online 23 JAN 2015

The effect of complex black carbon microphysics on the determination of the optical properties of brown carbon

Dantong Liu[1], Jonathan W. Taylor[1], Dominque E. Young[1], Michael J. Flynn[1], Hugh Coe[1], and James D. Allan[1,2]

[1]School of Earth, Atmospheric and Environmental Science, University of Manchester, Manchester, UK, [2]National Centre for Atmospheric Science, University of Manchester, Manchester, UK

Abstract Assessment of the impacts of brown carbon (BrC) requires accurate determination of its physical properties, but a model must be invoked to derive these from instrument data. Ambient measurements were made in London at a site influenced by traffic and solid fuel (principally wood) burning, apportioned by single particle soot photometer data and optical properties measured using multiwavelength photoacoustic spectroscopy. Two models were applied: a commonly used Mie model treating the particles as single-coated spheres and a Rayleigh-Debye-Gans approximation treating them as aggregates of smaller-coated monomers. The derived solid fuel BrC parameters at 405 nm were found to be highly sensitive to the model treatment, with a mass absorption cross section ranging from 0.47 to 1.81 m^2/g and imaginary refractive index from 0.013 to 0.062. This demonstrates that a detailed knowledge of particle morphology must be obtained and invoked to accurately parameterize BrC properties based on aerosol phase measurements.

1. Background

Optically absorbing soot in the atmosphere is characterized as being composed of a mixture of black carbon (BC) [*Bond et al.*, 2013] and brown carbon (BrC) [*Andreae and Gelencsér*, 2006]. These are both important to the radiative properties of the atmosphere but have different wavelength-dependent characteristics. Attempts to model the effect of BC and BrC are hindered by uncertainties in their fundamental properties. A key parameter governing the effect of BrC is the imaginary part (k_{BrC}) of the refractive index at short wavelengths, and a large range of values have been derived through field and laboratory studies, resulting in uncertainty surrounding its impacts [*Wang et al.*, 2014]. The absorption of brown carbon ($\sigma_{abs,BrC}$) from a variety of biomass burning sources has been assessed recently [e.g., *Lack et al.*, 2012; *Saleh et al.*, 2014] by subtracting the black carbon absorption ($\sigma_{abs,BC}$) from the total measured absorption ($\sigma_{abs,total}$). The explicit calculation of $\sigma_{abs,BC}$ is crucial for deriving $\sigma_{abs,BrC}$, and therefore its mass absorption cross section (MAC) and k_{BrC}. Therefore, the accuracy of the derived BrC parameters depends on the accuracy by which the BC properties can be estimated, which requires the invocation of an optical model treatment of the measured physical properties of the BC.

Mie-based models [*Bohren and Huffman*, 1983] has been widely used to model the absorption properties of particles by treating them as concentric spheres; however, this model may not apply for BC particles close to source regions as they often more resemble aggregates of many small monomers [e.g., *Xiong and Friedlander*, 2001; *China et al.*, 2013]. These aggregates can be described [*Filippov et al.*, 2000] by using parameters such as the fractal dimension (D_f), monomer diameter (D_s), and number of monomers (N_s), which forms the basis for a number of advanced models considering particle morphology, such as superposition T-matrix [*Mishchenko et al.*, 2013] and discrete dipole [*Adachi et al.*, 2010] models. A simplified approach, invoking Rayleigh-Debye-Gans (RDG) theory [*Bonczyk and Hall*, 1991], assumes that each monomer within the BC particle can serve as an independent light absorber and the total particle absorption is the sum of each monomer, based on which the MAC and absorption Ångström exponent (AAE) of the particle will thus entirely depend on the monomer. RDG has been shown to accurately predict optical properties for fresh, fractal-like BC particles [*Chakrabarty et al.*, 2007; *Adler et al.*, 2010], i.e., when $D_f < 2$ [*Bond and Bergstrom*, 2005].

The results presented in this study are obtained within the London urban environment during the winter season when the site was influenced by combined traffic and complex solid fuel burning sources [*Young et al.*, 2014b], and hence, a range of BC microphysics conditions are expected. Parameters for BC and BrC are derived

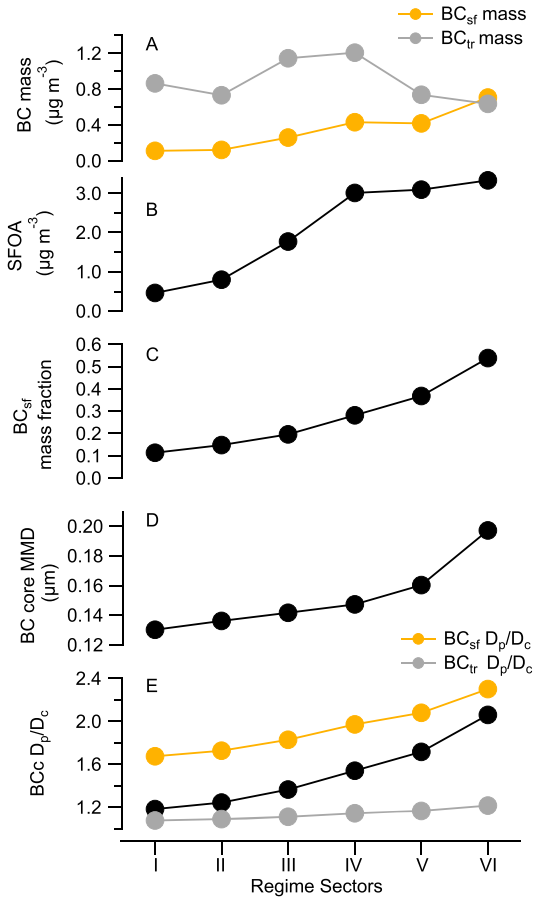

Figure 1. The average values of parameters for each regime sector (which are categorized by BC_{sf} mass fraction). (a to e) The BC mass, SFOA mass, BC_{sf} mass fraction, BC core MMD, and BCc D_p/D_c, respectively. Figure 1e shows the separated BC_{sf} and BC_{tr} coating thicknesses shown as brown and grey lines respectively, with black line showing the overall coating thickness.

and the modeling approach is varied in order to explore sensitivities in the derivation of these parameters. The results obtained using Mie and RDG are compared, as two extremes of the possible model treatments available (a single-uniform object versus many noninteracting objects).

2. Measurements and Data Analysis

The results presented in this study were obtained during winter 2012 as part of the Clean Air for London (ClearfLo) project [*Bohnenstengel et al.*, 2014]. The sources of BC mass from this study have been previously apportioned as BC from traffic (BC_{tr}) and from solid fuel burning (BC_{sf}) at the single-particle level using a single-particle soot photometer (Droplet Measurement Technologies (DMT), SP2) measurement [*Liu et al.*, 2014]. The SP2 measures the refractory BC (rBC) spherical equivalent core diameter (D_c) and the coating thickness (particle diameter, D_p, divided by the core diameter, D_p/D_c) for each particle. The term BC-containing particle (BCc) is used in the following text when referring to an entire particle containing rBC.

The methodology to determine the D_p/D_c is detailed in *Taylor et al.* [2014] and *Liu et al.* [2014]. The measured scattering cross section (C_{Sca}) of coated BC was fitted using a prescribed Mie lookup table at the SP2 operational wavelength $\lambda = 1064$ nm. Within the scope of this work, the effect of the particle geometry on the SP2 scattering response is also tested by applying the Rayleigh-Debye-Gans (RDG) approximation as an extreme case of fractal particle shape (Figure S1 and section S1 in the supporting information). The uncertainty of the derived D_p/D_c due to particle geometry is $<6\%$.

Figure S2 gives an overview of the BC and BrC related properties during the experiment, as reported by *Liu et al.* [2014]. The BC_{sf} has a larger coating thickness and larger rBC core compared to BC_{tr}. The environment is categorized by six regimes (denoted as I to VI) representing progressively increased contributions from BC_{sf}. The upper bound for the BC_{sf} mass fraction for regime I is the 10th percentile of all data points. Likewise, the 25th, 50th, 75th, and 90th percentiles are upper bounds for the other five regimes. Figure 1 shows the BC_{sf} mass fraction increases from 11% to 54% from regime I to VI. Over the same range of conditions, BC core mass median diameter (MMD) increases from 130 nm to 197 nm, particle bulk D_p/D_c increases from 1.19 to 2.04 with BC_{tr} showing a consistently low D_p/D_c and high D_p/D_c for BC_{sf} throughout the experiment, and the solid fuel organic aerosol (SFOA) mass loading increasing from 0.46 to 3.33 $\mu g\,m^{-3}$.

A thermodenuder (TD) [*Huffman et al.*, 2008] with an activated charcoal denuder downstream was operated at a maximum heating temperature of 250°C (referred to as TD250°C) to remove the volatile and semivolatile components in the sample. The SP2 sampled alternately between ambient air and air modified by the TD. Wavelength-dependent $\sigma_{abs,total}$ was measured by a photoacoustic soot spectrometer (PASS-3, DMT). The PASS-3 green (532 nm) channel was calibrated using absorbing polystyrene spheres referenced to NO_2 [*Lack et al.*, 2009]. The blue (405 nm) and red (781 nm) channels were matched to the green using denuded, traffic dominated data, assuming an absorption Ångström exponent (AAE) of unity [e.g., *Bergstrom et al.*, 2002; *Schnaiter et al.*, 2003; *Kirchstetter et al.*, 2004]. The MAC_{total} was obtained by a least squares linear

regression of the PASS measured $\sigma_{abs,total}$ and the SP2 measured rBC mass for the data subset in each regime, and for both ambient and TD250°C, as shown in section S3. The equivalent values downstream of the thermal denuder indicate that the coatings associated with BC have not been completely removed (Figure S3b) [also *Liu et al*., 2014, Figure 5], and the MAC_{total} follows an increasing trend when coating thickness is increased. Figure S3c shows the variations of MAC_{total} as a function of coating thickness for both ambient and TD250°C air are very similar, suggesting the SP2 measurement constrains the coating thickness under both conditions.

3. Modeling on BC Absorption Properties

A Mie model is applied to the SP2 single-particle data based on the BC core (D_c) size and coating thickness (section S4). The fraction for a successful detection of coating thickness by the SP2 drops below unity when D_c is smaller than 110 nm [*Liu et al*., 2014], which will bias the coating thickness data high in this size range; thus, the coating thickness (relative to core diameter) distribution in the D_c range 110–150 nm is extrapolated to particles with $D_c < 110$ nm. Figure S4 shows the Mie calculated $MAC_{BCc}(D_c)$ at each D_c bin size within each regime, which is then integrated over the entire D_c distribution to get the bulk MAC_{BCc} (section S4). From regime I to regime VI, the modeled bulk MAC_{BCc} becomes higher because of the increased coating thickness.

The choice of the BC core refractive index (n_{core}) will considerably modify the MAC value, and the n_{core} could be different for BC_{tr} and BC_{sf} and be dependent on λ. Given the main objective of this work is to explore the particle shape effect on modeled optical properties, a consistent n_{core} is assumed. In line with many other studies [e.g., *Lack et al*., 2012; *Adler et al*., 2010; *Bond and Bergstrom*, 2005], an $n_{core} = 1.85 + 0.71i$ and coating refractive index $n_{coat} = 1.5 + 0i$ are used at all λ. The BrC may be internally mixed with BC and so the coating will be absorbing, i.e., the $k_{coating}$ (the imaginary part of $n_{coating}$) is >0. Given the coatings are mixtures of organic and some other secondary nonabsorbing inorganic materials, an accurate $k_{coating}$ is unknown. We have tested the sensitivity of the calculation of absorption to $k_{coating}$ by varying the latter from 0 to 0.015 at blue wavelengths, at the extreme case of this study $D_p/D_c = 2.1$, the absorption at blue wavelengths is increased by less than 8%. Uncertainties in the measured mass and the diameters using the SP2 have previously been explored in *Liu et al*., 2014.

A Rayleigh-Debye-Gans (RDG) approximation is invoked to simulate the soot aggregate composed of coated monomers with varying sizes, as explained by equation (1).

$$\sigma_{abs} = N_s \times \sigma_{s,abs} \quad (1)$$

$$N_s = (D_c/D_s)^3 \quad (2)$$

where $\sigma_{s,abs}$ is the absorption coefficient of the monomer and N_s is the number of monomers in a single fractal particle, which is determined from the volume ratio of the core size to the monomer size using an assumed monomer diameter (D_s). The $\sigma_{s,abs}$ is calculated using Mie theory by applying the same particle bulk D_p/D_c to the monomer assuming the coating is evenly distributed on each monomer [*Adler et al*., 2010]. We make use of the source apportionment of BC mass at the single-particle level [*Liu et al*., 2014] to obtain separate optical treatments of BC_{tr} and BC_{sf}.

To test the λ sensitivity for both model approaches under different BC core sizes, the AAE is shown in Figure 2, for both uncoated BC and at the maximum coating thickness observed in this study ($D_p/D_c = 2.1$). For uncoated BC, the Mie modeled AAE_{Mie} converges to 1 when BC core diameter (D_c) is small, gradually rising up to $D_c \sim 100$ nm and sharply decreasing when D_c is larger than 120 nm. The observed D_c size range in this study (Figure 1d, 120–195 nm, as shown in grey bar in Figure 2) is exactly located in the regime where the AAE_{Mie} reduces markedly with core size; however, the monomer sizes used in the RDG calculation (as shown in grey vertical lines in Figure 2) lie in the regime where AAE_{RDG} increases. This phenomenon will lead to significant λ discrepancy between the Mie and RDG models, which can be expected because photons at shorter wavelengths will not penetrate the volume of a larger absorbing sphere as efficiently. This AAE discrepancy is more acute when BC is coated: increased coating thickness significantly increases the AAE_{RDG}; however, it only slightly decreases AAE_{Mie}. To summarize, a larger BC core size and thicker coating thickness will increase the λ discrepancy between Mie and RDG models.

The monomer diameter (D_s) of BC_{sf} is highly uncertain as there was no electron microscopy data at this site during the experiment, and the burning conditions were complex for the site during the wintertime [*Young*

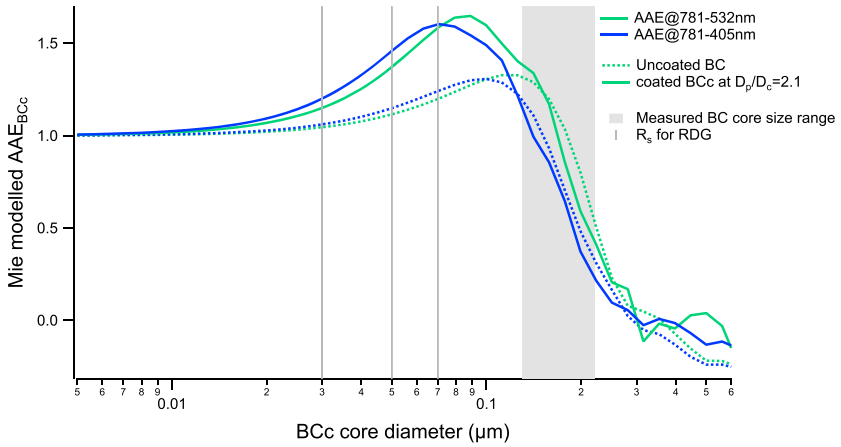

Figure 2. The AAE_{BCc} calculated by Mie as a function of BC core diameter, showing uncoated BC and coated BCc at $D_p/D_c = 2.1$; the grey bar denotes the measured MMD range observed in this study, and the three vertical grey lines are the chosen monomer diameters for RDG models.

et al., 2014b]. We therefore varied the monomer size of BC_{sf} ($D_s = 30$, 50, and 70 nm) to cover the range of monomer sizes found in the literature [*China et al*., 2013]. $D_s = 70$ nm is tested as a "worst case" because the modeled AAE reaches a maxima at the measured coating thickness, as shown in Figure 2. A narrower range of $D_s = 30$–50 nm for diesel soot is reported by previous studies [e.g., *Lammel and Novakov*, 1995; *Xiong and Friedlander*, 2001; *Braun et al*., 2004; *Vander Wal et al*., 2007; *Adler et al*., 2010], and it is assumed that this study is consistent with this. Given the BC_{tr} observed in this study is thinly coated throughout the experiment (Figure 1e), a D_s shifting from 30 to 50 nm leads to only a minor sensitivity to AAE. *Adler et al*. [2010] reported a best constrained model output using $D_s = 50$ nm for diesel soot, so we use this value for BC_{tr} for a more detailed sensitivity examination of the more complex BC_{sf}.

The BC cores may have not been completely embedded within the coating but may be attached on the surface or partly included in the coatings [e.g., *Adachi et al*., 2010]. To treat BC cores as complete concentric inclusions within entire particles will necessarily overestimate the coating enhancement on absorption [*Fuller et al*., 1999; *Bond et al*., 2006]. Therefore, in terms of BC microphysics, each of the models in this study will give an upper estimate for the absorption of coated BC.

4. Results and Discussion

The measured MAC_{total} derived from the ratio of the PASS and SP2 is shown together with the modeled MAC_{BCc} for different regimes in Figure 3. For particles exposed to TD250°C, it has not been possible to treat the BC_{sf} and BC_{tr} separately because the single-particle source apportionment fails when the original BC coating thickness is removed by the TD [see *Liu et al*., 2014, Figure 5a]; therefore, only $D_s = 50$ nm for all groups of particles is used when TD250°C. Figure 3b shows the RDG with $D_s = 50$ nm matches well with the measurement at all λ for regime I when the traffic source dominates.

Under all conditions, the Mie-modeled MAC_{BCc} is higher than the RDG-modeled MAC_{BCc} at $\lambda = 781$ nm and 532 nm. This is also manifested by a threshold BC core size test that above which the RDG-derived absorption is higher than that derived from the Mie: using the core refractive index $n_{core} = 1.85 + 0.71i$ and coating refractive index $n_{coat} = 1.5 + 0i$, for uncoated BC, RDG is only larger than Mie when $D_c > 390$ nm at $\lambda = 781$ nm, $D_c > 250$ nm at $\lambda = 532$ nm and $D_c > 190$ nm at $\lambda = 405$ nm; for coated BCc with $D_p/D_c = 2.1$, the threshold D_c to achieve RDG absorption greater than Mie absorption is enlarged to be 520 nm at $\lambda = 781$ nm, and 320 nm at $\lambda = 532$ nm, but the RDG absorption at $\lambda = 405$ nm is highly sensitive to the chosen monomer size at $D_p/D_c = 2.1$. For both ambient and TD250°C, at red wavelengths where BrC is deemed to be nonabsorbing, RDG matches better than Mie with the measurement, in agreement with previous studies that show that at λ_{red} RDG improves the prediction of optical properties compared to Mie for fractal flame soot [*Chakrabarty et al*., 2007].

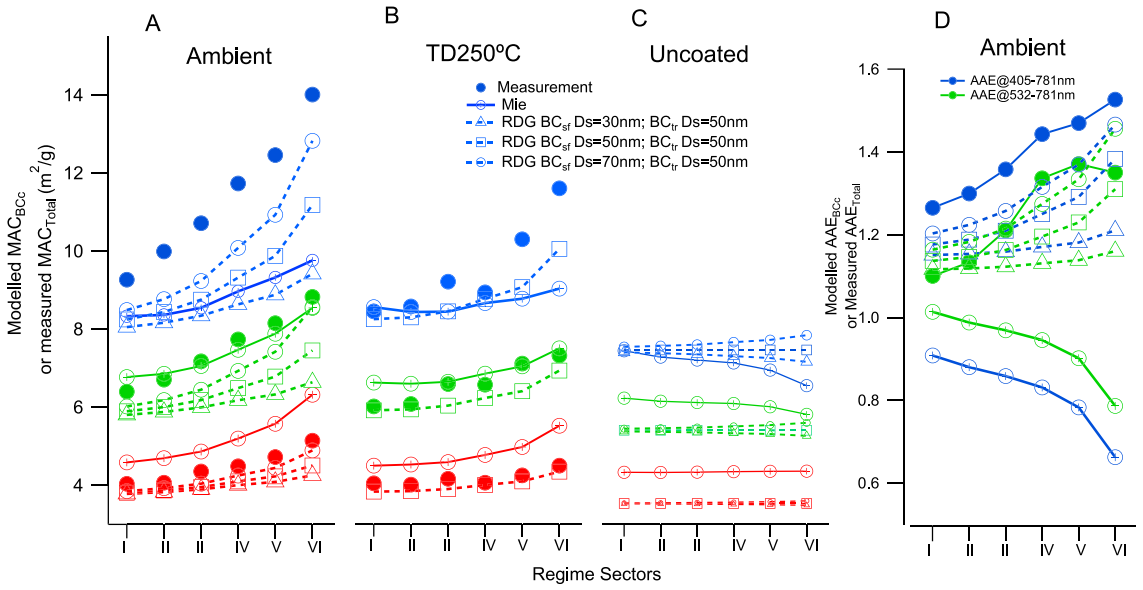

Figure 3. The measured MAC_{total} derived by PASS/SP2 and modeled MAC_{BC} by Mie and RDG. (a) For ambient, (b) for TD250°C (note that only $D_s = 50$ nm is used for RDG as the source apportionment was not available under this condition), and (c) for uncoated rBC core (model only). The blue, green, and red colors denote the PASS operational wavelengths at 405 nm, 532 nm, and 781 nm, respectively, and this color scheme is used throughout the main text and supporting information. Used in these calculations are $n_{core} = 1.85 + 0.71i$ and $n_{coat} = 1.50 + 0i$. (d) The modeled AAE_{BCc} and measured AAE_{total} for ambient data.

The difference between the measured MAC_{total} and modeled MAC_{BCc} is assumed to be the absorption of externally mixed BrC ($\sigma_{abs,BrC}$). At λ_{blue}, this difference does appear to be positive regardless of the model used, and it is noted that even at TD250°C, the $\sigma_{abs,BrC}$ still contributes. However, at λ_{green}, this is less well defined. A few studies [e.g., *Lack et al.*, 2012; *Adler et al.*, 2010] observed little or very weak $\sigma_{abs,BrC}$ at green λ, although *Saleh et al.* [2014] reported $k_{BrC} = 0.01–0.04$ at $\lambda = 550$ nm.

From regime I to regime VI, the modeled MAC_{BCc} for both ambient and TD250°C increases because of the increased coating thickness (Figure S3b); however, the trend in increasing MAC_{BCc} calculated using the Mie model becomes lower at λ_{blue}, because of the decreasing AAE_{Mie} (Figure 3d) with increasing BC core size. The discrepancy between Mie and RDG becomes progressively larger from regions I to VI, and the RDG output is highly sensitive to the chosen monomer size. These results are all consistent with the model predicted AAE (Figure 2), and, as shown in Figure 3d, an increase of BC core size and coating thickness increases the discrepancy between Mie and RDG.

Some fraction of the BrC mass may have been internally mixed within BC containing particles. A simplified approach is conducted to estimate this fraction assuming the SFOA mass fraction contributing to the BC coating is the same as that in the whole ambient particle population. Given this assumption, a fraction of 0.7–0.8 of SFOA is estimated to be externally mixed with BC, which is consistent with *Lack et al.* [2012], who found about 80% of the BrC is externally mixed. A MAC_{BrC} was then obtained by dividing the $\sigma_{abs,BrC}$ with the externally mixed BrC mass, which is then input into the Mie model to get k_{BrC}. As Figure S5 and Table 1 show, for regime VI when BC_{sf} contributes about 54% of the BC mass, the model discrepancies can lead to MAC_{BrC} ranging from 0.47 to 1.81 m^2/g (a factor of ~3.8 uncertainty) and the resulting k_{BrC} ranges from 0.013 to 0.062 (a factor of ~4.7 uncertainty) at $\lambda = 405$ nm.

Table 1. The BrC Optical Parameters for Regime VI as Calculated by Different Model Approaches

BrC Optical Parameters	Mie	RDG With BC_{sf} $D_s = 30$ nm	RDG With BC_{sf} $D_s = 50$ nm	RDG With BC_{sf} $D_s = 70$ nm
$MAC_{BrC}(m^2/g)$	1.68	1.81	1.11	0.47
k_{BrC}	0.056	0.062	0.033	0.013

The discrepancy between RDG and Mie essentially reflects a particle shape effect on the optical properties. Fresh diesel soot particles have been long established to be fractal. A recent transmission electron microscopy (TEM) study [*China et al*., 2013] revealed that fresh wildfire soot is also highly fractal with $D_f = 1.53–1.92$ despite the high organic coatings present which may act to collapse the core; therefore, it cannot be assumed that Mie is appropriate for this aerosol type. A few laboratory studies [e.g., *Cross et al*., 2010; *Zhang et al*., 2008] have shown that very thick coatings on aged soot particles or after the coatings are thermodenuded lead to compaction of the particles. The complex morphology of BC may vary with time with varying BC sources and aging times: although this is impossible to be examined in real time during this study, it is clear that neither the Mie nor RDG models provide a complete model description of the optical properties but nevertheless provide two extreme constraints on the effect of particle shape. This study was conducted in urban London during winter season when the particles were mainly primary and the aging timescales tended to be short [*Young et al*., 2014a]. It is therefore expected that the BC particles observed in this study are thus closer to a more fractal shape.

To date many experimental studies have used Mie modeling to represent BrC optical properties, and this representation is used in large-scale model studies with the optical parameters of BrC still bearing large uncertainties [*Wang et al*., 2014]. The optical properties of carbonaceous aerosols have been largely derived from the measurements close to sources assuming simplified soot morphology [e.g., *Saleh et al*., 2014; *Lack et al*., 2012]. This study highlights the importance of particle morphology on affecting the model sensitivity and the extent to which such uncertainty away from source regions remains to be explored. A model framework for accurately describing ambient BC optical properties is not yet available and needs to address these considerable uncertainties that presently exist.

5. Conclusions

This study uses measurements of single-particle black carbon mass containing mixed traffic and solid fuel (SF) burning sources to evaluate the performance of optical models when applied to deriving key parameters governing BC and BrC absorption. A simple Mie-based approach, as used in previous publications, was compared against a Rayleigh-Debeye-Gans approximation of complex aggregates, with the monomer sizes varied to investigate sensitivity. Large discrepancies among model results at shorter wavelength are found when SF sources dominate due to the larger BC core size and thicker coating thickness. A BC mass fraction from SF of 54% led to a factor of ~3.8 difference in MAC_{BrC} (from 0.47 to 1.81 m^2/g) derived from Mie and RDG models and a factor of ~4.7 difference in k_{BrC} (from 0.013 to 0.062) derived from the two approaches. This large discrepancy can be explained as a high sensitivity of BC absorption Ångström Exponent (AAE_{BC}) to the BC core size. If a spherical BC core is assumed for the BC mass, a core diameter of 110–200 nm has been derived for a range of traffic and biomass burning sources [e.g., *Liu et al*., 2014; *McMeeking et al*., 2010; *Schwarz et al*., 2008; *Kondo et al*., 2011]. At these sizes, the Mie calculated AAE_{BC} reduces markedly with size. However, if the BC particle is made up of a number of smaller spherules, a much larger AAE_{BC} will be derived. This sensitivity is most acute for larger core sizes and thickly coatings, such as those commonly observed in BC particles from biomass burning sources, and may be lessened for smaller and thinly coated BC from fresh traffic sources. The use of Mie calculation, which assume the freshly emitted biomass burning BC acts as solid sphere, tends to underestimate the AAE_{BC} and so causes the BrC absorption parameters to be overestimated at shorter wavelengths. Advanced models, such as the superposition T-matrix [*Mishchenko et al*., 2013] and discrete dipole [*Adachi et al*., 2010] models require explicit characterization of BC microphysics, such as the monomer size and BC core position relative to the host coatings, although deriving specific parameters for complex burn conditions will be challenging.

Acknowledgments
This work was supported through the UK Natural Environment Research Council (NERC) through the MC4 (grant reference NE/H008136/1) and ClearfLo (grant reference NE/H003150/1) projects. Processed data are available through the ClearfLo project archive at the British Atmospheric Data Centre (http://badc.nerc.ac.uk/browse/badc/clearflo). Raw data are archived at the University of Manchester and are available on request.

The Editor thanks two anonymous reviewers for their assistance in evaluating this paper.

References

Adachi, K., S. H. Chung, and P. R. Buseck (2010), Shapes of soot aerosol particles and implications for their effects on climate, *J. Geophys. Res.*, *115*, D15206, doi:10.1029/2009JD012868.

Adler, G., A. A. Riziq, C. Erlick, and Y. Rudich (2010), Effect of intrinsic organic carbon on the optical properties of fresh diesel soot, *Proc. Natl. Acad. Sci. U.S.A.*, *107*, 6699–6704.

Andreae, M. O., and A. Gelencsér (2006), Black carbon or brown carbon? The nature of light-absorbing carbonaceous aerosols, *Atmos. Chem. Phys.*, *6*, 3131–3148, doi:10.5194/acp-6-3131-2006.

Bergstrom, R. W., P. B. Russell, and P. Hignett (2002), The wavelength dependence of black carbon particles: Predictions and results from the Tarfox experiment and implications for the aerosols single scatter albedo, *J. Atmos. Sci.*, *59*, 567–577.

Bohnenstengel, S. I., et al. (2014) Meteorology, air quality, and health in London: The ClearfLo project, *Bull. Am. Meteorol. Soc.*, ISSN 1520-0477, doi:10.1175/BAMS-D-12-00245.1.

Bohren, C. F., and D. R. Huffman (1983), *Absorption and Scattering of Light by Small Particles*, Wiley, Weinheim, Germany.
Bonczyk, P. A., and R. J. Hall (1991), Fractal properties of soot agglomerates, *Langmuir*, *7*(6), 1274–1280.
Bond, T. C., and R. W. Bergstrom (2005), Light absorption by carbonaceous particles: An investigative review, *Aerosol Sci. Technol.*, *40*, 27–67.
Bond, T. C., G. Habib, and R. W. Bergstrom (2006), Limitations in the enhancement of visible light absorption due to mixing state, *J. Geophys. Res.*, *111*, D20211, doi:10.1029/2006JD007315.
Bond, T. C., et al. (2013), Bounding the role of black carbon in the climate system: A scientific assessment, *J. Geophys. Res. Atmos.*, *118*, 5380–5552, doi:10.1002/jgrd.50171.
Braun, A., F. E. Huggins, S. Seifert, J. Ilavsky, N. Shah, K. E. Kelly, A. Sarofim, and G. P. Huffman (2004), Size-range analysis of diesel soot with ultra-small angle X-ray scattering, *Combust. Flame*, *137*(1), 63–72.
Chakrabarty, R. K., H. Moosmüller, W. P. Arnott, M. A. Garro, J. G. Slowik, E. S. Cross, J. H. Han, P. Davidovits, T. B. Onasch, and D. R. Wornsop (2007), Light scattering and absorption by fractal-like carbonaceous chain aggregates: Comparison of theories and experiment, *Appl. Opt.*, *46*, 6990–7006.
China, S., C. Mazzoleni, K. Gorkowski, A. C. Aiken, and M. K. Dubey (2013), Morphology and mixing state of individual freshly emitted wildfire carbonaceous particles, *Nat. Comm.*, *4*, 2122, doi:10.1038/ncomms3122.
Cross, E. S., et al. (2010), Soot particle studies-instrument inter-comparison—Project overview, *Aerosol Sci. Technol.*, *44*(8), 592–611.
Filippov, A. V., M. Zurita, and D. E. Rosner (2000), Fractal like aggregates: Relation between morphology and physical properties, *J. Colloid Interface Sci.*, *229*, 261–273.
Fuller, K. A., W. C. Malm, and S. M. Kreidenweis (1999), Effects of mixing on extinction by carbonaceous particles, *J. Geophys. Res.*, *104*(D13), 15,941–15,954.
Huffman, J. A., P. J. Ziemann, J. T. Jayne, D. R. Worsnop, and J. L. Jimenez (2008), Development and characterization of a fast-stepping/scanning thermodenuder for chemically-resolved aerosol volatility measurements, *Aerosol Sci. Technol.*, *42*, 395–407.
Kirchstetter, T. W., T. Novakov, and P. V. Hobbs (2004), Evidence that the spectral dependence of light absorption by Aerosols is affected by organic carbon, *J. Geophys. Res.*, *109*, D21208, doi:10.1029/2004JD004999.
Kondo, Y., et al. (2011), Emissions of black carbon, organic, and inorganic aerosols from biomass burning in North America and Asia in 2008, *J. Geophys. Res.*, *116*, D08204, doi:10.1029/2010JD015152.
Lack, D. A., et al. (2009), Absorption enhancement of coated absorbing aerosols: Validation of the photo-acoustic technique for measuring the enhancement, *Aerosol Sci. Technol.*, *43*, 1006–1012, doi:10.1080/02786820903117932.
Lack, D. A., J. M. Langridge, R. Bahreini, C. D. Cappa, and A. M. Middlebrook (2012), Brown carbon and internal mixing in biomass burning particles, *Proc. Natl. Acad. Sci. U.S.A.*, *109*, 14,802–14,807.
Lammel, G., and T. Novakov (1995), Water nucleation properties of carbon-black and diesel soot particles, *Atmos. Environ.*, *29*(7), 813–823.
Liu, D., et al. (2014), Size distribution, mixing state and source apportionment of black carbon aerosol in London during wintertime, *Atmos. Chem. Phys.*, *14*, 10,061–10,084, doi:10.5194/acp-14-10061-2014.
McMeeking, G. R., et al. (2010), Black carbon measurements in the boundary layer over western and northern Europe, *Atmos. Chem. Phys.*, *10*, 9393–9414, doi:10.5194/acp-10-9393-2010.
Mishchenko, M. I., L. Liu, and D. W. Mackowski (2013), T-matrix modeling of linear depolarization by morphologically complex soot and soot-containing aerosols, *J. Quant. Spectrosc. Radiat. Transfer*, *123*, 135–144, doi:10.1016/j.jqsrt.2012.11.012.
Saleh, R., et al. (2014), Brownness of organics in aerosols from biomass burning linked to their black carbon content, *Nat. Geosci.*, *7*, 647–650.
Schnaiter, M., H. Horvath, O. Möhler, K.-H. Naumann, H. Saathoff, and O. Schöck (2003), UV-VIS-NIR spectral optical properties of soot and soot-containing aerosols, *J. Aerosol Sci.*, *34*(10), 1421–1444.
Schwarz, J. P., et al. (2008), Measurement of the mixing state, mass, and optical size of individual black carbon particles in urban and biomass burning emissions, *Geophys. Res. Lett.*, *35*, L13810, doi:10.1029/2008GL033968.
Taylor, J. W., J. D. Allan, D. Liu, M. Flynn, R. Weber, X. Zhang, B. L. Lefer, N. Grossberg, J. Flynn, and H. Coe (2014), Assessment of the sensitivity of core/shell parameters derived using the single particle soot photometer to density and refractive index, *Atmos. Meas. Tech. Discuss.*, *7*, 5491–5532, doi:10.5194/amtd-7-5491-2014.
Vander Wal, R. L., A. Yezerets, N. W. Currier, D. H. Kim, and C. M. Wang (2007), HRTEM Study of diesel soot collected from diesel particulate filters, *Carbon*, *45*(1), 70–77.
Wang, X., C. L. Heald, D. A. Ridley, J. P. Schwarz, J. R. Spackman, A. E. Perring, H. Coe, D. Liu, and A. D. Clarke (2014), Exploiting simultaneous observational constraints on mass and absorption to estimate the global direct radiative forcing of black carbon and brown carbon, *Atmos. Chem. Phys.*, *14*, 10,989–11,010, doi:10.5194/acp-14-10989-2014.
Xiong, C., and S. K. Friedlander (2001), Morphological properties of atmospheric aerosol aggregates, *Proc. Natl. Acad. Sci.*, *98*(21), 11,851–11,856.
Young, D. E., J. D. Allan, P. I. Williams, D. C. Green, M. J. Flynn, R. M. Harrison, J. Yin, M. W. Gallagher, and H. Coe (2014a), Investigating the annual behaviour of submicron secondary inorganic and organic aerosols in London, *Atmos. Chem. Phys. Discuss.*, *14*, 18,739–18,784, doi:10.5194/acpd-14-18739-2014.
Young, D. E., J. D. Allan, P. I. Williams, D. C. Green, R. M. Harrison, J. Yin, M. J. Flynn, M. W. Gallagher, and H. Coe (2014b), Investigating the two-component model of solid fuel organic aerosol in London: Processes, PM1 contributions, and seasonality, *Atmos. Chem. Phys. Discuss.*, *14*, 20,845–20,882, doi:10.5194/acpd-14-20845-2014.
Zhang, R. Y., A. F. Khalizov, J. Pagels, D. Zhang, H. Xue, and P. H. McMurry (2008), Variability in morphology, hygroscopicity, and optical properties of soot aerosols during atmospheric processing, *Proc. Natl. Acad. Sci. U.S.A.*, *105*, 10,291–10,296, doi:10.1073/pnas.0804860105.